Soil Environ. 44(1): 18-27, 2025
DOI: doi.org/10.25252/SE/2025/253522
Online ISSN: 2075-1141
Print ISSN: 2074-9546

Phenol adsorption onto orange peel biochar from aqueous solution: Isotherm study

Meenal Iqbal[1], Kiran Hina[1*], Usman Ghani[1] and Muhammad Ibrahim[2]
[1]Department of Environmental Science, University of Gujrat, Gujrat Pakistan 50700
[2]Department of Environmental Sciences, Government College University, Faisalabad-38000, Pakistan
***[Received:** August 19, 2024 **Accepted:** March 10, 2025 **Published Online:** March 27, 2025]*

Abstract

In this study adsorption isotherms of orange peel biochar (Citrus sinesis) for removal of phenol from the aqueous solution were investigated. Orange peel biochar (OPB) having different particle sizes: 1, 3, and 5 mm (post pyrolysis) was produced at different pyrolysis temperatures i.e. 350, 450, and 550 ℃, (OPB350, OPB 450 and OPB550). Our Findings showed that surface chemistry of OPB varied greatly with pyrolysis temperature-rise in terms of aromatic functional groups and structural properties. Operating parameters i.e. adsorption reaction time (10-180 min), adsorbent dose (0.5-3 g) and phenol concentration (100-400 mg L^{-1}) were studied. Our findinngs exhibited that phenol adsorption on biochar surfaces catalyzed at high pyrolysis temperature and particle size of 3 mm. Adsorption results indicate that the adsorption capacity of OPB reduced with high initial concentration and reached 98.3% with an increase in contact time (up to 120 minutes) afterward a declining trend was noted. It is evident from the findings of current investigation that OPB proved to be good adsorbent for phenol removal. The highest (98%) of phenol removal was observed at a lower initial concentration with OPB550 having 3 mm particle size whereas the minimal removal was noticed with OPB produced at lower pyrolysis temperature (OPB350) having 1 mm particle size. This is mainly attributed to less attachment sites on biochar surfaces and biochar particles become clogged. Adsorption isotherms followed Langmuir model with R^2 values of 0.99, 0.992 and 0.987 for OPB350, OPB450 and, OPB550, respectively.

Keywords: Adsorption, orange peel biochar, pyrolysis temperature, particle size, phenol

Introduction

Increased industrialization has escalated the production of polluted water. Continuous discharge of pollutants particulary phenol in water bodies deteriorates the quality of water (Zhu *et al*., 2020). Phenol is a hazardous organic pollutant which is very toxic to all living creatures even at very low concentrations (Kadhum *et al*., 2021). Phenol is widely used in many industries as part of many processes that resulted in significant water contamination when discharged into water bodies (Dhote *et al*., 2012). Long term exposure of phenol to humans causes fatal diseases like anorexia, diarrhea, salivation, dark urine discoloration, liver, blood and gastrointestinal tract abnormalities *etc*. (Das *et al*., 2014). It also interferes human metabolism by transforming its shape very immediately by reacting with different quinone residues that form covalent bonds with proteins (Dias *et al*., 2021). The discharge limit of phenol in water bodies is 1 ppb and in drinking-water should not exceed 0.001 ppm (Mandal *et al*., 2020). Phenol has persistent nature, poor biodegradability and damages human health even at lower concentrations. Therefore, considering its wide use and hazardous nature, phenol removal from wastewater has attained substantial interest before discharging into water-bodies for human safety and ecosystem protection. Many methods such as solvent extraction, bio-degradation, adsorption process, polymerization, membrane separation, ultrasonic degradation and photo-catalysis *etc*. have been developed and employed to remove phenol from wastewater (Adak *et al*., 2006). Adsorption process stands out pertinent due to its cost-effectiveness *i.e*. simplicity, high absorption capacity, environmental friendly nature and regeneration possibilities *etc.* (Zhang *et al*., 2018). Biosorption is primarily done by using naturally available ingredients such as fruit waste, sawdust, rice husk, coconut husks, poultry manure and other tannin-rich materials (Inyang and

***Email:** kiran.hina@uog.edu.pk
Cite This Paper: Iqbal, M., K. Hina, U. Ghani and M. Ibrahim. 2025. Phenol adsorption onto orange peel biochar from aqueous solution: Isotherm study. 44(1): 18-27.

Dickenson, 2015; Mohammed *et al*., 2018; Saeed *et al*., 2020; Ghani *et al*., 2022). When a material with an exceptional porous surface comes into contact with an adsorbable solution, intermolecular interactions between the liquid and solid surface cause solution's solute molecules to concentrate or become adsorbed on the surface of solid material (Villegas *et al*., 2016). It is a broadly used process owing to its simple design and operation (Hussain *et al*., 2015; Godwin *et al*., 2019). The carbonaceous material formed by thermal conversion of orange peels in oxygen-deficient media. Biochar is a very cheap and widely used material that is used as a multifunctional material for wastewater remediation but it is important to make relevant biochar keeping in view the nature of target organic pollutant. Biochar has large surface area, diverse functional groups, and porous structure which determines its performance (Kang *et al*., 2019; Oh and Seo, 2019; Varjani *et al*., 2019). The adsorption capacity of biochar is improved by combining it with the other materials like iron, acids, and minerals *etc*. to make it more effective in adosrptiom of pollutants (Xiang *et al*., 2020). The characteristics of pristine biochar depends on multiple factors, such as feedstock type, preparation protocols *i.e*. heating rate, time, particle size, and pyrolytic temperature but these conditions are easy to ensure and inexpensive which is why it is preferred (Samsudin *et al*., 2019). For instance, sugarcane biochar is used to remove 2,4,6-trichlorophenol in the concentrated solutions as an efficient and cost-effective adsorbent (Mubarik *et al*., 2016). The micro-porous surface of softwood biochar plays pivotal role in adsorption process. To decrease pentachlorophenol, rice straw biochar was used by Luo *et al*. (2015). Municipal bio-solids are pyrolzed to produce biochar and used to remove the halogenated phenol (Oh and Seo, 2016). The meta-analysis showed the less environmental impacts of biochar during synthesis process than activated carbons (Arshad *et al*., 2017). Slow pyrolysis method outweighs the other methods in terms of commercial point and sorbent properties such as carbon content, porosity and chemical and biological stability (Mubarik *et al*., 2016).

The current study aimed to produce low-cost adsorbent using the food waste, namely the orange peels and investigate its adsorption isotherms in removing phenol from the aqueous solution due to its aforementioned hazardous and persistent nature. In developing countries i.e. Pakistan orange fruit are common and produce food waste at large scale. Biochar was produced by slow pyrolysis method at 350, 450, and 550 °C temperatures as well as at different particle sizes . The particular focus is to compare and investigate the adsorption capacities and effect of pyrolysis temperature on the adsorption behavior.

Materials and Methods

Biochar preparation and characterization

The orange peels (*Citrus sinesis*) were collected from clean fields of Gujrat, Pakistan. Initially, sun-dried orange peels were oven-dried at 80 ℃ for 2 hours and washed with distilled water (DI) for removal of impurities. The feedstock material was taken in a porcelain dish and pyrolyzed in a muffle furnace (Thermoscientific™ FB1310M) at different temperatures 350, 450, and 550 ℃ for 3 hrs under reduced oxygen supply conditions (furnace was pre heated to desired temperature for reduced oxygen supply) and then left for cooling at room temperature. The obtained biochar was named as OPB350, OPB450, and OPB550. The dried orange peel biochars were ground to pass through a different pore size sieves to get different sizes of biochar 1, 3 and 5mm. After cooling, the biochar was rinsed with DI followed by oven drying at 80 °C. The prepared orange peel biochar samples were characterized by different advanced analytical techniques. Scanning electron microscope (SEM; Hitachi S-3000N, Hitachi scientific instruments, Tokyo, Japan) was used to evaluate the surface structure and the functional groups on biochar were analyzed through Fourier transforms infrared spectroscopy (Model: FTIR Spectrum 100 PerkinElmer) at scan rate of 4000 to 350 cm^{-1} .

Batch experiment

A stock solution (500 mg L^{-1}) was prepared by means of analytical-grade phenol crystals; (Shalimar Scientific Store). The working solution was made directly from the stock solution to the required concentration with distilled water. Batch experiments were conducted using 250 mL flask at neutral pH with 100 mg L^{-1} phenol solutions in orbital shake at 120 rotations per minute. In all experiments, 150 mL of phenol solution was mixed with 2 g adsorbent except effect of biochar dosage. After the anticipated contact time, the mixed solution was withdrawn and placed in centrifugation tubes at 1000 rpm for 5 min; filtered, and supernatant was analyzed by UV visible spectroscopy (UV1700, Shimadzu, Japan) and the calibration curve was used to calculate effluent concentration. Different factors *i.e.* reaction time, biochar dose and phenol concentration were studied. To assess reaction time effect on the adsorption efficiency, the samples were collected at intervals of 10, 30, 60, 90, 120, 150 and 180 min and for biochar dose effect, the working samples were fed by the different doses of adsorbent (0.5-3 g). The effect of phenol concentration was conducted by using 100, 200, 300 and, 400 mg L^{-1} and the supernatant was analyzed

through UV vis. spectrophotometer (UV1700, Shimadzu, Japan).

Isotherm study

The phenol removal and adsorption capacity of OPB was used as an evaluation indicator for the performance of adsorbent. The removal percentage of adsorption was calculated from Eq. (1).

$$\%R = \frac{(Ci-Ce)}{Ci} \times 100 \quad (1)$$

Maximum adsorption capacity Qe (mg g^{-1}) of phenol was computed by using Eq. (2).

$$Qe = \frac{(Ci-Ce)\times V}{m} \quad (2)$$

where *Ci* and *Ce* are the initial and final phenol concentration (mg L^{-1}) and *V* is solution volume (L) and m is the weight of added adsorbent (g). The Langmuir, Freundlich, and Tempkin models were plotted for isotherms studies and removal efficiencies of both adsorbents were analyzed using Eq. (3), (4), and (5) below, respectively.

$$\frac{1}{qe} = \frac{1}{KLqmax}.\frac{1}{Ce} + \frac{1}{qmax} \quad (3)$$

$$Logqe = LogKf + \frac{1}{n}LogCe \quad (4)$$

$$qe = \frac{RT}{bT}lnAT + \left(\frac{RT}{bT}\right)lnCe \quad (5)$$

where q_{max} (mg g^{-1}) is the maximum adsorption capacity, K_L (L mg^{-1}) Langmuir constant associated with the attraction between a biochar and phenol, the value of q_{max} and K_L determined from the graph slope and intercept of Langmuir plot 1/Ce vs. 1/1/qe; Kf (mg g^{-1} or L mg^{-1}) Freundlich constant, which determines the adsorption strength, n (dimensionless) is a intensity parameter, AT is Tempkin isotherm equilibrium binding constant (L g^{-1}), bT Tempkin

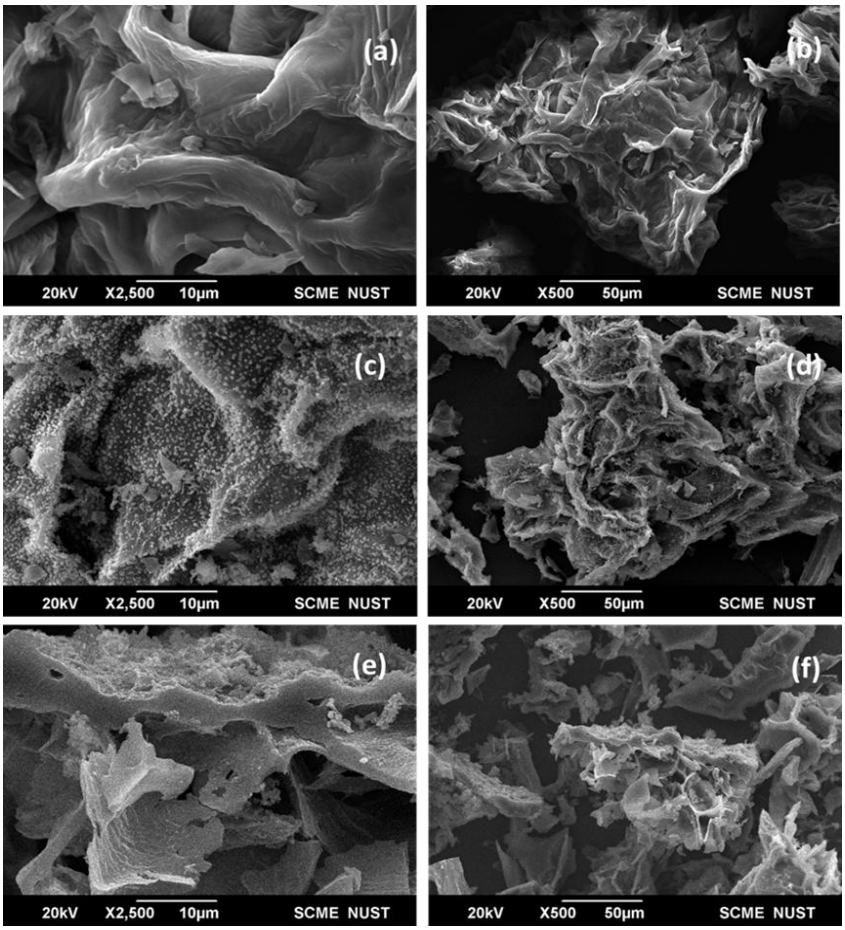

Figure 1: SEM images of OPB 350 (a, b), OPB 450 (c, d), and OPB 550 (e, f)

constant, R is the universal gas constant (8.314 J mol^{-1} K^{-1}), T is temperature 298 K.

Results and Discussion

Scanning electron microscopy of biochar

To analyze morphology and structural characteristics of the manufactured biochar SEM analysis was done. SEM figures are very helpful for more accurate and better understanding of the surface structure of OPB. The figures revealed that surface of OPB prepared at 350, 450, and 550°C, are smooth and flower-like (Figure 1(a) and (b)). The biochar surfaces have a heterogeneous morphology of smaller particles, which might be attributed to secondary char depositions from orange peel's highly volatile matter concentration (Figure 1(c) and (d)). The evident brittling surface and porosity proved the procalamation and volatilization of volatile matter and lignocellulosic material (Figure 1 (e), (f)). Instead of releasing volatiles quickly, slow pyrolysis promotes the development of micropores. With its rough, uneven surface and heterogeneously dispersed cavities (Zhao *et al*., 2020), biochar has the potential to promote adsorption in aqueous media, as well as improve the adsorption of compounds like phenol. Further, the enormous size of the holes interprets large top areas and improved the adsorptive capability of burn matter. Though, this can be stopped by the lower burn matter removal. The pair splitting of the tarry mixture and more curing might perform important work in the making of carbon pledge, leading to hole closed and lessening pores (Shin, 2017). The pores of burn matter change the physical structure of burn material permanently which eventually affects the sample process temperature. The OPB is used as an absorbent material for the treatment of polluted water, as of bundle-like hole form which performs essential work in the removal of many harmful pollutants (Nguyen and Oh, 2019). These should also be matched to the tiny shape reactor, warranting further formational tests with various step-up reactor kinds.

Fourier transmission infrared spectroscopy of biochar

The properties of OPB like surface area and rough structures are very important to check their acceptability for pollutants attachment. In Figure 2, various infrared bands of OPB are shown which are referred to many functional groups based on their relative wave-number (cm^{-1}) as described in earlier studies. The -OH groups produce a significant peak ranging between 3600 cm^{-1} which becomes less severe between OPB350 and OPB550 samples. Similarly, the small sets of peaks at 2900 cm^{-1} indicate a drop in sp-3 C-H bonding, which is seen at 600 °C and is analogous to the decrease in saturated carbons (Mondal *et al*., 2021). In contrast, the OPB350, OPB450, and OPB550 biochar corresponds to replace in cyclic rings with a high concentration of small peaks at wave-number smaller than 900 cm^{-1}, resulting in increasing aromaticity of the biochar at high temperature. Because of the loss of functional groups caused by reduced carbonization, the FTIR spectra for the OPB350 samples were noticeably flatter.

In OPB350, a significant absorption peak was observed just above 1600 cm^{-1}, which was linked to carboxylic acid groups (Figure 2a). In OPB550, a more dominant absorption was observed at 1000-1200 cm^{-1} which could be associated with phenol groups. These groups are responsible for the known hydroxyl absorption, as well as for the small peaks visible at 1400 cm^{-1} (Figure 2c). Tiny peaks at 1500-1600 cm^{-1} observed in OPB350 and OPB450, indicate N-O expands with nitro components. Between 2200 and 23400 cm^{-1}, a significant fragile peak (compared to 350 and 450 °C) showed double bonding of carbon with carbon, nitrogen, and oxygen groups, and reviewed the increasing proportion of this bonding [Figure 2. (a) and (b)]. The accessibility of strong functional groups on the OPB is linked to the form of adsorption onto biomass materials. An FTIR spectral examination was performed to explain these energetic sites. The aliphatic C-H stretching (methane, methyl, and methylene groups on side chains) is responsible for the fragile band visible at about 2900 cm^{-1} (Tran *et al*., 2019). The CO stretching in ketones, aldehydes or carboxyl groups occurs around 1700 cm^{-1}, while the C=C to and fro movement in aromatic rings occurs in the band between 1600 and 1500 cm^{-1} (Qambrani *et al*., 2017). In oxidized carbon materials, bands between 1300 and 1000 cm^{-1} are linked with C-O and C-O-C stretching in acids, phenols, ethers, and esters groups as well as sulphonic acids groups ($-SO_3$) (Zhang *et al*., 2017). As a result, the outer surface of OPB has many functional groups including carboxylic and carbonyl oxygen, as shown by its FTIR spectrum of OPB in the adsorption process.

Factors affecting adsorption capacity

Effect of time

In this work, various time intervals (10-180 min) were studied to check the quantity of phenol adsorbed on OPB350, OPB450 and OPB550. The phenol adsorptions by orange peel biochar at different pyrolysis temperatures (350, 450, 550 °C) and particle sizes (1, 3, and 5 mm) are shown in Figure 3(a–c). Adsorption was completed in 120 mins at a low phenol concentration 100 mg L^{-1}, and the equilibrium was settled in the solution. During the 90 mins reaction period, phenol adsorption on OPB350, OPB450 and OPB550

reached 6.31, 5.96 and 6.51 mg g^{-1} while at 120 minutes it was 6.88, 6.75 and 7.38 mg g^{-1}, respectively. when the contact duration was 120 minutes, the maximum percentage of phenol adsorption for OPB350, OPB450, and OPB550 were 91.66, 90.053, and 98.37%, respectively. This shows a rising behavior of phenol adsorption at high temperature and smaller particle sizes at a certain contact time period. In contrast to the findings of Lee *et al*. (2019), increase in phenol sorption from 10.91±0.13 mg g^{-1} to 12.63±0.16 mg g^{-1} at 24h was credited to presence of active sites on OPB surface (Idrees *et al*., 2018).

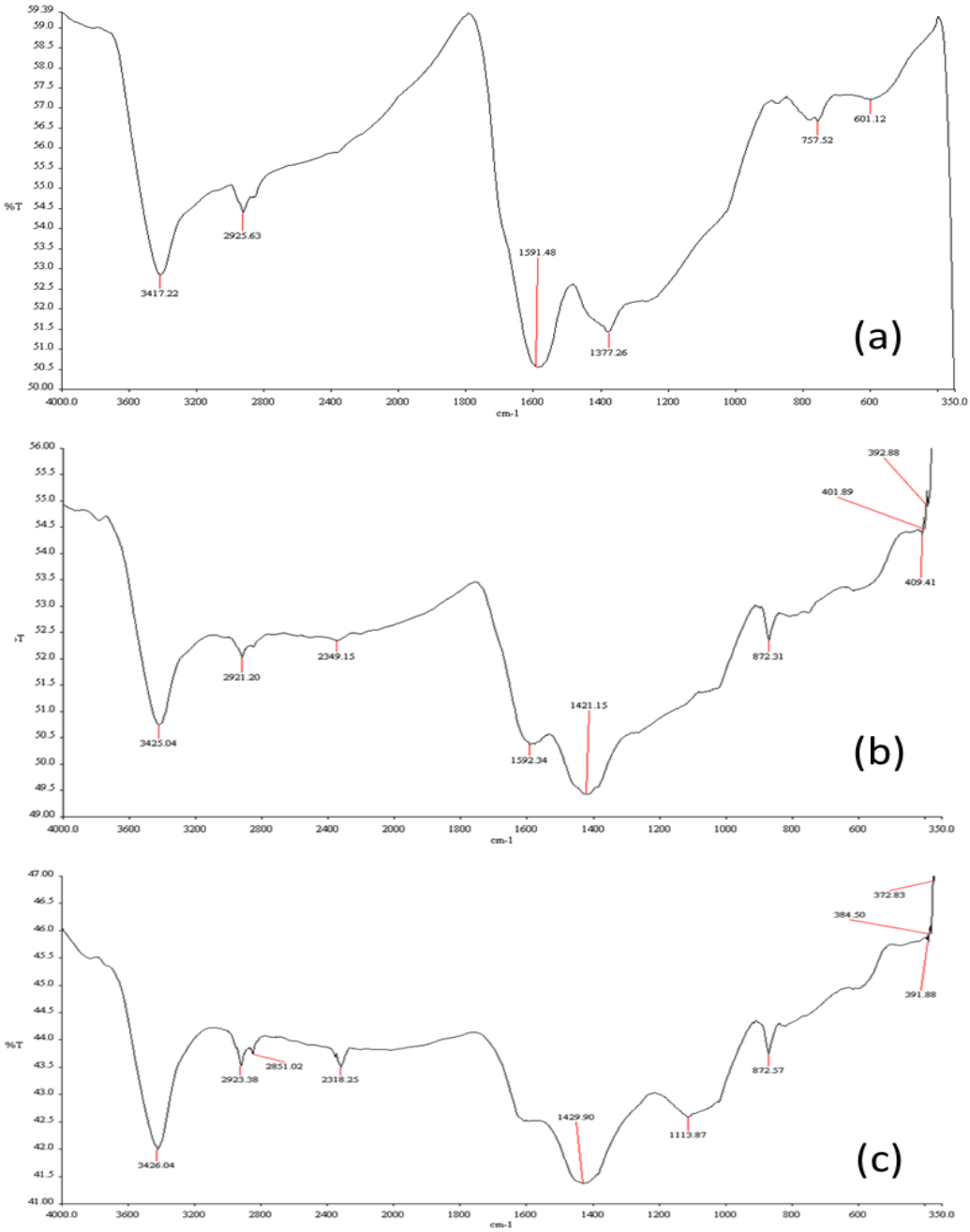

Figure 2: FTIR images of OPB350 (a), OPB450 (b), and OPB550 (c)

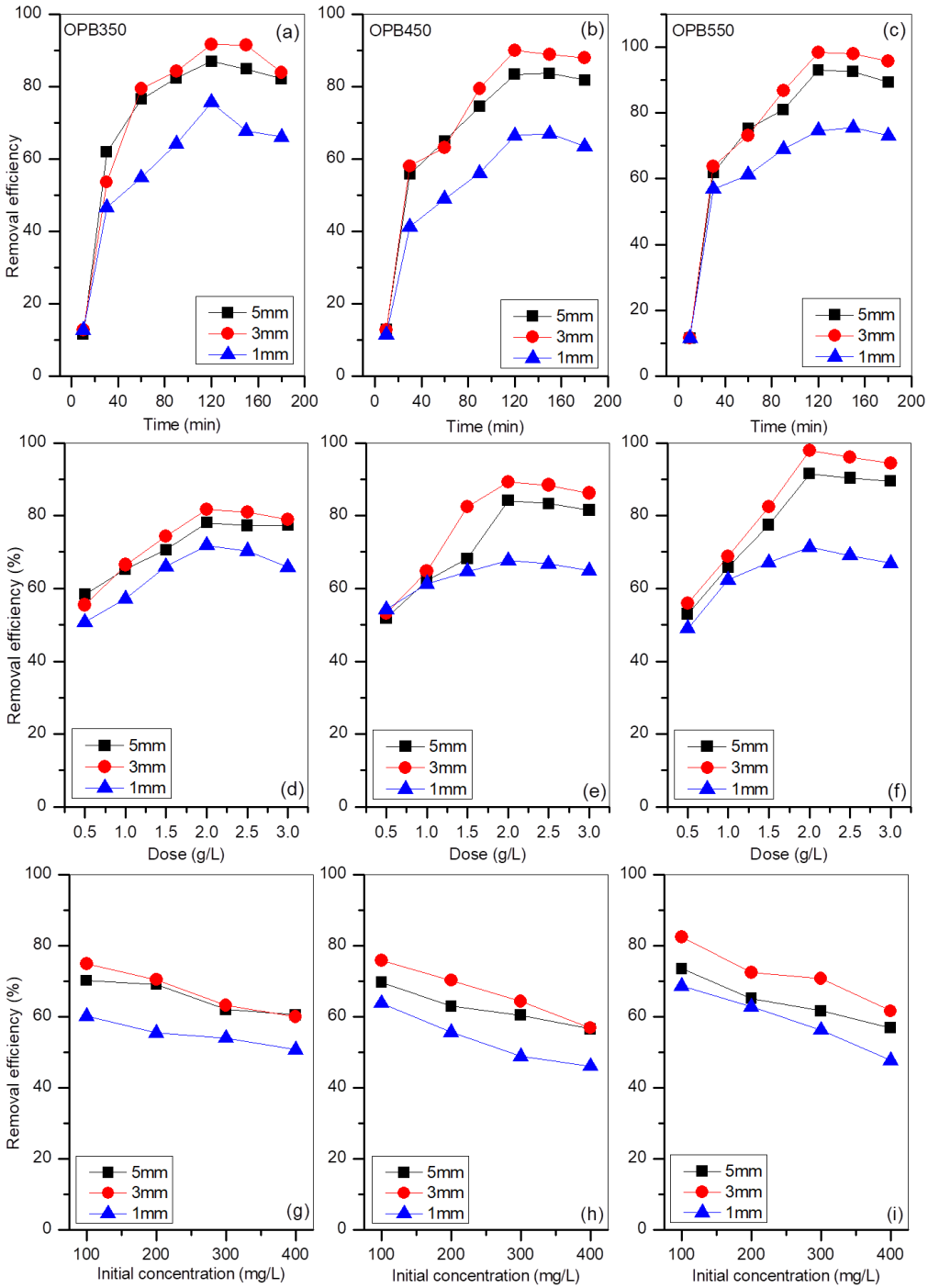

Figure 1: Effect of time (a-c), dose (d-f), and initial concentration (g-i) on Removal efficiency

Effect of dose

Figure 3(d–f), shows the sorbent dose behavior. For this purpose, experiments were conducted by using different quantities of sorbent (0.5–3.0 g). Whereas other parameters remained same like 100 mg L^{-1} of initial concentration, 150 rpm for 120 min at room temperature. The obtained experimental results revealed that maximum adsorption reached above 81.66, 89.28 and 97.8% for OPB350, OPB450 and OPB550 at the dose of 2 g of sorbent, respectively, while further addition of sorbent did not contribute to elevating the adsorption efficiency. Our results interpreted that high efficiency was due to increased available active sites for phenol adhesion. Beyond 2.0 g adsorbent dose in 100 mL solution, no important phenol adsorption was noticed because of limited number of active sites. Based on obtained results, 2 g sorbent dose was selected as optimum condition for subsequent experimentation. The adsorption trend went above the 97 % removal under 120 min reaction. These results can be validated by the findings of Lee *et al*. (2019) who concluded that rising adsorbent dose from 0.1 g to 0.5 g adsorption efficiency improved but up to a limit, while further addition of sorbent caused a reduction in adsorption efficiency with corresponding values of 9.91 ± 0.52 to 5.02 ± 0.06 mg g^{-1}, which clearly demonstrate increase in the removal efficiency(90.7%) after increasing adsorbent dose to 0.6 g (Irfan *et al*., 2014; Gao *et al*., 2019).

Effect of initial concentration

Figure 3(g–i) revealed phenol adsorption behavior on OPB at various initial concentrations. The quantity of adsorbed phenol enhanced vastly through OPB350 adsorbent from 5.62 to 18.0 mg g^{-1} and OPB550 from 6.18 to 18.50 mg g^{-1} as phenol concentration rose from 100 to 400 mg L^{-1}. The reason is the driving force which is more smoothly controlled to hinder the mass shifting around the solid and liquid state. At higher phenol concentrations, removal was attributed to a higher attachment of phenol onto OPB surface. Consequently, high phenolic ions attach OPB surface because it tended to infiltrate into the inner surface of the OPB and adsorbed at active pore sites but it took longer to achieve equilibrium for high adsorption. This shows that the phenol concentration has a major effect on adsorption

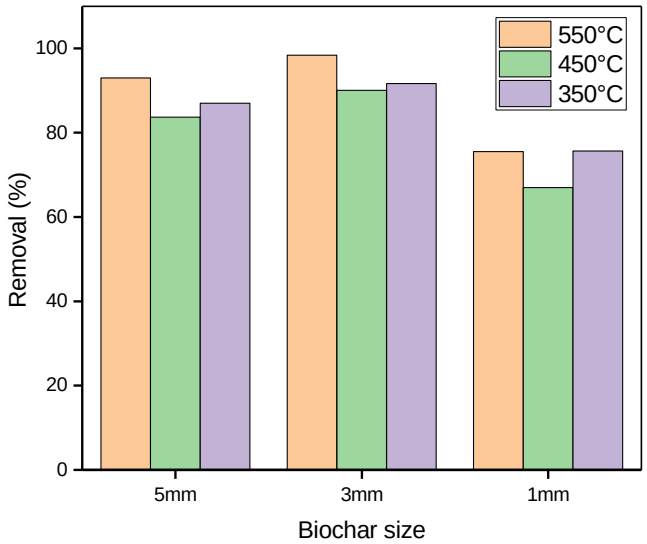

Figure 4: Comparison of removal efficiency of biochar produced at different particle size and pyrolysis tempratures

Table 1: Langmuir, Freundlich and Tempkin constant values for phenol adsorption on OPB350, OPB450 and OPB550

Adsorbent	Langmuir isotherms				Freundlich isotherms			Tempkin isotherms		
	q_{max} (mg g^{-1})	K_L	R_L	R^2	K_f	1/n	R^2	BT (J mol^{-1})	KT (L mg^{-1})	R^2
OPB350	41.44	0.0049	0.669	0.99	13.58	-0.753	0.860	-3.086	0.033	0.907
OPB450	28.98	0.0072	0.5825	0.992	13.78	-0.753	0.956	-3.025	0.029	0.973
OPB550	24.41	0.011	0.479	0.987	8.195	-0.506	0.833	-2.439	0.037	0.870

capability of OPB sorbent. The main force between OPB and phenol increases as phenol concentration rises, while the overall efficiency decreases but the adsorption quantity increases (Lee *et al*., 2017; Idrees *et al*., 2018). The removal percentage increased at the initial concentration 100 mg L^{-1} at 2 g L^{-1} of OPB but as phenol concentration enhanced from 100 to 400 mg L^{-1}, it reduced from 82.42% to 61.66% of OPB550. In contrast with experiments executed by (Samsudin *et al*., 2019), the phenol adsorption performance of FWC700 increased with phenol concentration reaching 4.34 ± 0.90 mg g^{-1}. Literature reported that initial concentration increasing from 10 to 200 mg L^{-1} increased the phenol and DNP adsorption rate was decreased from 98.8% to 80.5% (Carvajal-Bernal *et al*., 2015). Prior studies described that the adsorption ability decreases due to less active sites and surfaces on the top of the sorbent due to an increase in the quantity of environmental contamination (Oh and Seo, 2016; Shakoor *et al*., 2016; Oh and Seo, 2019; Varjani *et al*., 2019).

Comparison analysis

Figure 4 shows that different particle sizes and pyrolysis temperatures of OPB have a powerful impact on adsorption capacity. As temperature rises from 350 to 550 °C the phenol removal onto OPB also rose with the value of 91.66, 90.053, and 98.37%, respectively. When the sizes of particles were reduced to 1 mm, the removal efficiency also decreased to 75.5%. It is because of agglomeration of biochar particles and become clogged surface which lead to reduction in number of active sites on sorbent surface for phenol attachment (Lee *et al*., 2019).

Adsorption mechanism

The removal of phenol by OPB can be explained by following mechanisms; surface adsorption, hydrogen bond formation and second π–π interaction. First the phenol molecules are physically adsorbed on the OPB surface via weak Vander Waal forces and second the hydrogen bond formation can be explained by oxygenated functional groups (=O, -OH, -COOH, O=C-H) which prohibited the π–π interaction between phenol and surface of biochar and lead to hydrogen bond formation with phenol molecules. This phenol adsorption mechanism validated the irreversible adsorption by strong electrostatic attraction. The phenol adsorption mechanism can be explained by π–π interaction by which electrons of phenol ring react with aromatic strucures present on surface of biochar.

Adsorption isotherms

The adsorption with different phenol concentrations was analyzed using the linear Freundlich (Eq. 3), Langmuir (Eq. 4) and Tempkin models (Eq. 5) in which Ce equilibrium concentration of, K_f and 1/n are the Freundlich constants related to the adsorption capacity and intensity and, K_L is Langmuir constant belongs to the attraction of the attachment site, AT (L g^{-1}) is Tempkin constant in sequence. Table-1 showed the model fitting parameters. The dimensionless separation factor of the Langmuir adsorption process is described as follows: 0.670, 0.48, and 0.583 for OPB350, OPB450 and, OPB550, respectively, which was calculated using the phenol concentration (100 mg L^{-1}). Values between 0 and 1 indicated that phenol adsorption on biochar are adequate (Bekkouche *et al*., 2012; Zhou *et al*., 2016). The maximum adsorption capacity (q_{max}) of OPB550 calculated from Langmuir isotherm was 28.98 mg g^{-1}, while previously reported study had maximum adsorption capacity of biochar with values of 14.04 mg g^{-1} to 83.88 mg g^{-1} (Shin, 2017) and commercial activated carbon was also compared with OPB under the same experimental conditions, and the activated carbon's maximum adsorption capacity for phenol was 67.19 ± 4.90 mg g^{-1} according to the Langmuir model. The plots were the Langmuir isotherm model Ce versus Ce/qe (Figure 5a-c), as well as the slope and intercept plots of logCe against logqe for the Freundlich model (Figure 5d-f) and lnCe for the Tempkin model (Figure 5g-i). According to the Langmuir model, Phenol's correlation coefficient (R^2) of OPB550 was higher (R^2<0.99), than the Freundlich isotherm model (R^2>*0.83*) and Tempkin isotherm model (R^2>0.87). The Langmuir isotherm model had a greater relative correlation coefficient, indicating that monolayer phenolic adsorption on OPB. Our findings further revealed that Phenol adsorption on OPB followed a uni-layer adsorptive process through a homogeneous distribution of activated sites. These indicated that a uni-layer of adsorbate has developed on the adsorbent's surface, with no additional adsorption once the active surface has been completely covered (Bardestani *et al*., 2019).

Currently, the residual products of forest and agriculture have been used as a substitute sorbent for the adsorption of phenol from the liquid mixture. The highest q_{max} value of many biochars produced from different feedstocks for phenol removal was observed which were higher than the values found in this study, including the bamboo biomass biochar (166.7 mg g^{-1}), pine fruit shell (26.7 mg g^{-1}) and granulated cork (0.9 mg g^{-1}), rice husk (14.4 mg g^{-1}) and rice straw (80.5 mg g^{-1}), coconut shell biochar (19.9 mg g^{-1}) and commercial activated carbon (69.9 mg g^{-1}). This indicates that OPB might be a good adsorbent for removing phenol from wastewater. The Freundlich isotherm assumed a multi-layer adsorption technique on a heterogeneous surface with uneven adsorption heat. The constant K_f represents the phenol adsorption

capacity when exposed to OPB. Table-1 revealed that the K_f values of Phenol were 13.58, 13.78, and 8.195, respectively.

By contrast to the Langmuir structure, the same order of adsorption capability is absorbed with the Freundlich pattern, which has a lower relationship constant of observed data. Furthermore, the value of 1/n should be established as both works of adsorption capacity and different standards (if 1/n = 1, adsorption is linear; 1/n > 1, chemical; and 1/n < 1, adsorption is a physical favorable process). The non-similarity factor (1/n) were -0.753, -0.753, and -0.506, respectively. When seeing the Tempkin isotherm constant value R^2 of OPB350 and OPB450 is higher than OPB550, it can be said that the Tempkin isotherm model is also well adequate for phenol adsorption. The results depicted that phenol adsorption onto OPB occurs in physical adsorption

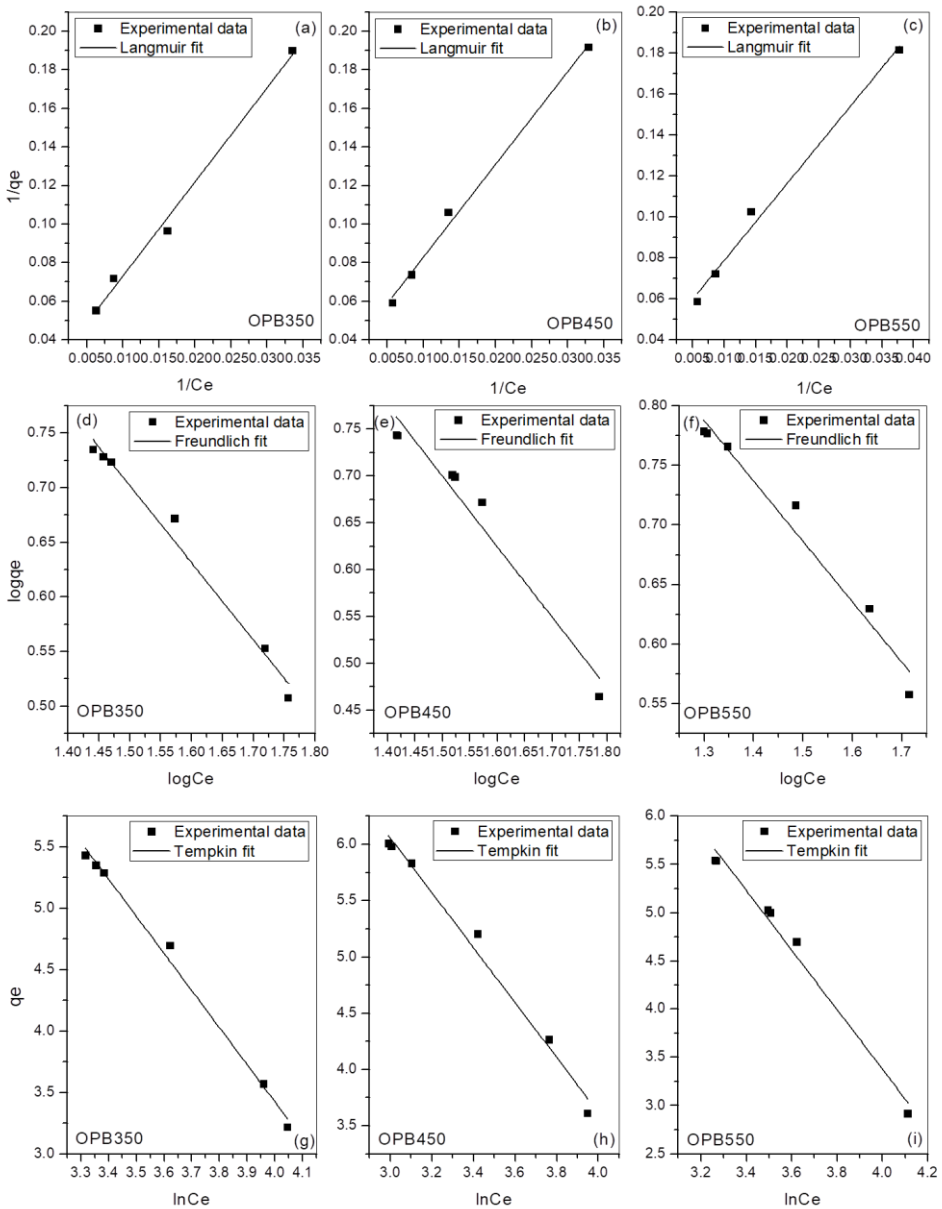

Figure 5: Adsorption isotherms (a-c) Langmuir, (d-f) Freundlich and (g-i) Tempkin model

manner, and Langmuir isotherm is a best fitting isotherm than the Freundlich isotherm (Pan and An, 2019; Zeng *et al*., 2019).

Conclusions

This study showed that OPB production cost is less than commercial activated carbon. The reason of low cost is that orange peels were easily available waste in Pakistan and only cost involved was the price of electricity used to run the muffle furnace. The power supply needed to run furnace was minimal, thereby OPB production was economical to produce and use in wastewater treatment. Moreover, findings of current study illustrated that surface functional groups, and structural roughness of OPB become diverse with increasing pyrolysis temperature. Phenol adsorption on OPB increased with high pyrolysis temperature and 3 mm particle size. The surface functional groups and structure of OPB were all positively associated with adsorption behavior. The availability of active sites on OPB surface could justify the high adsorption efficiency. The OPB arise as a good adsorbent for phenol removal as the percentage phenol removal efficiency is 98% at lower phenol concentration with 3 mm particle size and 550 °C pyrolysis temperature. This was due to clogging of biochar particles. Langmuir isotherm model well fitted with the experimental data with R^2 values of 0.99, 0.992 and 0.987 for OPB350, OPB450 and OPB550, respectively. This study explored the adsorption behavior of OPB and its useful application for environmental remediation. The biochar obtained from food waste can be used as efficient and ecomonical sorbent material for the removal of phenol from aqueous solution.

References

Abdelhafez, A.A. and J. Li. 2016. Removal of Pb (II) from aqueous solution by using biochars derived from sugar cane bagasse and orange peel. *Journal of the Taiwan Institute of Chemical Engineers* 61: 367-375.

Adak, A., A. Pal and M. Bandyopadhyay. 2006. Removal of phenol from water environment by surfactant-modified alumina through adsolubilization. *Colloids and Surfaces A: Physicochemical and Engineering Aspects* 277: 63-68.

Arshad, M., A.H.A Khan, I. Hussain, M. Anees, M. Iqbal, G. Soja, C. Linde and S. Yousaf. 2017. The reduction of chromium (VI) phytotoxicity and phytoavailability to wheat (*Triticum aestivum* L.) using biochar and bacteria. *Applied Soil Ecology* 114: 90-98.

Bardestani, R., C. Roy and S. Kaliaguine. 2019. The effect of biochar mild air oxidation on the optimization of lead (II) adsorption from wastewater. *Journal of Environmental Management* 240: 404-420.

Bekkouche, S., S. Baup, M. Bouhelassa, S. Molina-Boisseau and C. Petrier. 2012. Competitive adsorption of phenol and heavy metal ions onto titanium dioxide (Dugussa P25). *Desalination and Water Treatment* 37: 364-372.

Carvajal-Bernal, A.M., F. Gómez, L. Giraldo and J.C. Moreno-Piraján. 2015. Adsorption of phenol and 2, 4-dinitrophenol on activated carbons with surface modifications. *Microporous and Mesoporous Materials* 209: 150-156.

Das, S., R. Raj, N. Mangwani, H.R. Dash and J. Chakraborty. 2014. Heavy metals and hydrocarbons: Adverse effects and mechanism of toxicity. *Microbial Biodegradation and Bioremediation* 23-54.

Dhote, J., S. Ingole and A. Chavhan. 2012. Review on wastewater treatment technologies. *International journal of engineering research & technology* 1: 1-10.

Dias, R., H. Oliveira, I. Fernandes, J. Simal-Gandara and R. Perez-Gregorio. 2021. Recent advances in extracting phenolic compounds from food and their use in disease prevention and as cosmetics. *Critical Reviews in Food Science and Nutrition* 61: 1130-1151.

Gao, Q., J. Xu and X-H. Bu. 2019. Recent advances about metal–organic frameworks in the removal of pollutants from wastewater. *Coordination Chemistry Reviews* 378: 17-31.

Ghani, U., A. Idrees, K. Hina, M. Iqbal, M. Ibrahim, R. Saeed, M.K. Irshad, I. Aslam and W. Jiang. 2022. Adsorption of Methyl Orange and Cr (VI) onto Poultry Manure-Derived Biochar from aqueous solution. *Frontiers in Environmental Science* 644.

Godwin, P.M., Y. Pan, H. Xiao and M.T. Afzal. 2019. Progress in preparation and application of modified biochar for improving heavy metal ion removal from wastewater. *Journal of Bioresources and Bioproducts* 4: 31-42.

Hussain, K.I., M. Usman, M. Siddiq, N. Rasool, T.H. Bokhari, M. Ibrahim, U.A. Rana and S.U.D Khan. 2015. Application of micellar-enhanced ultrafiltration for the removal of reactive blue 19 from aqueous media. *Journal of Dispersion Science and Technology* 36: 1208-1215.

Idrees, M., S. Batool, , T. Kalsoom, S. Yasmeen, A. Kalsoom, S. Raina, Q. Zhuang and J.Kong. 2018. Animal manure-derived biochars produced via fast pyrolysis for the removal of divalent copper from aqueous media. *Journal of Environmental Management* 213: 109-118.

Inyang, M. and E. Dickenson. 2015. The potential role of biochar in the removal of organic and microbial contaminants from potable and reuse water: A review. *Chemosphere* 134: 232-240.

Irfan, M., M. Usman, A. Mansha, N. Rasool, M.Ibrahim, U.A. Rana, M. Siddiq, M. Zia-Ul-Haq, H.Z. Jaafar and S.U.D. Khan. 2014. Thermodynamic and spectroscopic investigation of interactions between reactive red 223 and

reactive orange 122 anionic dyes and cetyltrimethyl ammonium bromide (CTAB) cationic surfactant in aqueous solution. *The Scientific World Journal 2014 (1): (2014): 540975.The Scientific World Journal* 2014.

Kadhum, S.T., G.Y. Alkindi and T.M. Albayati. 2021. Eco friendly adsorbents for removal of phenol from aqueous solution employing nanoparticle zero-valent iron synthesized from modified green tea bio-waste and supported on silty clay. Chinese *Journal of Chemical Engineering* 36: 19-28.

Kang, S., G.Kim, J.K. Choe and Y. Choi. 2019. Effect of using powdered biochar and surfactant on desorption and biodegradability of phenanthrene sorbed to biochar. *Journal of Hazardous Materials* 371: 253-260.

Lee, C-G., S-H. Hong, S-G. Hong, J-W. Choi and S.J. Park. 2019. Production of biochar from food waste and its application for phenol removal from aqueous solution. *Water, Air, & Soil Pollution* 230: 1-13.

Lee, J., Y.F. Tsang, S. Kim, Y.S. Ok and E.E. Kwon. 2017. Energy density enhancement via pyrolysis of paper mill sludge using CO_2. *Journal of CO_2 Utilization* 17: 305-311.

Luo, L., C. Xu, Z. Chen and S. Zhang. 2015. Properties of biomass-derived biochars: Combined effects of operating conditions and biomass types. *Bioresource Technology* 192: 83-89.

Mandal, A., P. Mukhopadhyay and S.K. Das. 2020. Adsorptive removal of phenol from wastewater using guava tree bark. *Environmental Science and Pollution Research* 27: 23937-23949.

Mohammed, N.A., R.A. Abu-Zurayk, I. Hamadneh and A.H. Al-Dujaili. 2018. Phenol adsorption on biochar prepared from the pine fruit shells: Equilibrium, kinetic and thermodynamics studies. *Journal of Environmental Management* 226: 377-385.

Mondal, S., C.Vinod and U.K.Gautam. 2021. 'Autophagy'and unique aerial oxygen harvesting properties exhibited by highly photocatalytic carbon quantum dots. *Carbon* 181: 16-27.

Mubarik, S., A. Saeed, M. Athar and D.M. Iqbal. 2016. Characterization and mechanism of the adsorptive removal of 2, 4, 6-trichlorophenol by biochar prepared from sugarcane baggase. *Journal of Industrial and Engineering Chemistry* 33: 115-121.

Nguyen, T.H.A. and S.Y. Oh. 2019. Biochar-mediated oxidation of phenol by persulfate activated with zero-valent iron. J*ournal of Chemical Technology & Biotechnology* 94: 3932-3940.

Oh, S-Y. and Y.D. Seo. 2016. Sorption of halogenated phenols and pharmaceuticals to biochar: Affecting factors and mechanisms. *Environmental Science and Pollution Research* 23: 951-961.

Oh, S-Y. and Y.D. Seo. 2019. Factors affecting the sorption of halogenated phenols onto polymer/biomass-derived biochar: Effects of pH, hydrophobicity, and deprotonation. *Journal of Environmental Management* 232: 145-152.

Pan, Z. and L. An. 2019. Removal of heavy metal from wastewater using ion exchange membranes. p. 25-46. In: *Applications of Ion Exchange Materials in the Environment.* Inamuddin, M. Ahamed and A. Asiri (eds.) *Springer, Cham.*

Qambrani, N.A., M.M. Rahman, S. Won, S. Shim and C. Ra. 2017. Biochar properties and eco-friendly applications for climate change mitigation, waste management, and wastewater treatment: A review. *Renewable and Sustainable Energy Reviews* 79: 255-273.

Saeed, M., M. Siddique, M. Ibrahim, N. Akram, M. Usman, M.A. Aleem and A. Baig. 2020. *Calotropis gigantea* leaves assisted biosynthesis of ZnO and Ag@ ZnO catalysts for degradation of rhodamine B dye in aqueous medium. *Environmental Progress & Sustainable Energy* 39: e13408.

Samsudin, M.F.R., N. Bacho, S. Sufian and Y.H. Ng. 2019. Photocatalytic degradation of phenol wastewater over Z-scheme g-C3N4/CNT/BiVO4 heterostructure photocatalyst under solar light irradiation. *Journal of Molecular Liquids* 277: 977-988.

Shakoor, H., M. Ibrahim, M. Usman, M. Adrees, M.A. Mehmood, F. Abbas, N. Rasool and U. Rashid. 2016. Removal of Reactive Blue 21 from aqueous solution by sorption and solubilization in micellar media. *Journal of Dispersion Science and Technology* 37: 144-154.

Shin, W.S. 2017. Adsorption characteristics of phenol and heavy metals on biochar from *Hizikia fusiformis*. *Environmental EarthSciences* 76: 1-9.

Tran, C.H., L.T.T. Pham, Y. Lee, H.B. Jang, S. Kim and I.Kim. 2019. Mechanistic insights on Zn (II)− Co (III) double metal cyanide-catalyzed ring-opening polymerization of epoxides. *Journal of Catalysis* 372: 86-102.

Varjani, S., G. Kumar and E.R.Rene. 2019. Developments in biochar application for pesticide remediation: Current nowledge and future research directions. *Journal of Environmental Management* 232: 505-513.

Villegas, L.G.C., N. Mashhadi, M. Chen, D. Mukherjee, K.E. Taylor and N.Biswas. 2016. A short review of techniques for phenol removal from wastewater. *Current Pollution Reports* 2: 157-167.

Xiang, W., X. Zhang, J. Chen, W. Zou, F. He, X.Hu, D.C.Tsang, Y.S. Ok and B.Gao. 2020. Biochar technology in wastewater treatment: A critical Review. *Chemosphere* 252: 126539.

Yu, W., F. Lian, G. Cui and Z. Liu. 2018. N-doping effectively enhances the adsorption capacity of biochar for heavy metal ions from aqueous solution. *Chemosphere* 193: 8-16.

Zeng, T., E.R. Rene, S. Zhang, and P.N.Lens. 2019. Removal of selenate and cadmium by anaerobic granular sludge: EPS characterization and microbial community analysis. *Process Safety and Environmental Protection* 126: 150-159.

Zhang, C., B.Shan, W. Tang and Y.Zhu. 2017. Comparison of cadmium and lead sorption by Phyllostachys pubescens biochar produced under a low-oxygen pyrolysis atmosphere. *Bioresource Technology* 238: 352-360.

Zhang, S., X.Yang, L.Liu, M. Ju and K.Zheng. 2018. Adsorption behavior of selective recognition functionalized biochar to Cd (II) in wastewater. *Materials* 11: 299.

Zhao, C., S.Zhong, C. Li, H. Zhou and S. Zhang. 2020. Property and mechanism of phenol degradation by biochar activated persulfate. *Journal of Materials Research and Technology* 9: 601-609.

Zhou, L., Y. Liu, S. Liu, Y. Yin, G. Zeng, X. Tan, X. Hu, X.Hu, L.Jiang and Y. Ding. 2016. Investigation of the adsorption-reduction mechanisms of hexavalent chromium by ramie biochars of different pyrolytic temperatures. *Bioresource Technology* 218: 351-359.

Zhu, B., T. Wang, M. Dzakpasu and X. Li. 2020. Nutrient dynamics and retention in a vegetated drainage ditch receiving nutrient-rich sewage at low temperatures. *Science of The Total Environment* 741: 140268.